Fast pressure probe measurements of a high-velocity plasma plume

S. Messer,[a] A. Case, R. Bomgardner, M. Phillips, and F. D. Witherspoon
HyperV Technologies Corp., Chantilly, Virginia 20151, USA

(Received 10 April 2009; accepted 13 May 2009; published online 3 June 2009)

This article reports measurements of stagnation pressure on a contoured coaxial gun, now installed at the Maryland Centrifugal Experiment [R. Ellis *et al.*, Phys. Plasmas **12**, 055704 (2005)]. The impact of the plasma on the stationary probe is consistent with adiabatic compression and supersonic flow. Measured pressure signals are consistent with a shock traveling at 110 km/s and a following flow with speed of 90 km/s. At late times, the pressure profile is consistent with an adiabatically expanding plasma that fills the vacuum chamber. © *2009 American Institute of Physics*. [DOI: 10.1063/1.3148338]

Coaxial plasma accelerators ("Marshall guns")[1] are widely used to drive high-velocity and high-mass plasma flows.[2] These devices are in development for control of density[3] and velocity profiles, for refueling magnetic-confinement fusion experiments,[4] for space propulsion,[5–7] and for studies of magnetic fields,[8] turbulence, and instabilities[9] in plasmas. One of the limitations of coaxial plasma guns is the development of the blow-by instability.[10–12] We seek to mitigate this instability by the use of contoured inner and outer electrodes.[13] In this paper we describe measurements of the ram pressure due to the gun plasma plume. These results focus on data obtained from a fast piezoelectric pressure probe.

Our pressure probe is built around a PCB Piezotronics model 113A21 piezoelectric sensor. This sensor is encased in a 9.5 mm outer-diameter quartz tube to protect it from electrical and thermal damage by the plasma and to allow the probe to be moved relative to the vacuum chamber wall. The gun-facing end of the sensor is covered by a 0.5 mm thick quartz disk with a diameter of 10 mm (see Fig. 1). The assembled probe has been calibrated inside a rigid shock tube.[14,15] It gives a response of 2.28×10^{-6} V/Pa. Its initial rise time is about 0.6 μs, but it has a strong 160 kHz acoustic resonance. Interpretation is therefore problematic for any signals lasting less than about 2.4 μs. For our experiment, this probe gives signals on the order of 0.3 V and substantial acoustic oscillations during the approximately 10 μs pulse.

We collect pressure probe data at several axial locations downstream of the gun muzzle. At least five shots were taken at each position. For each trace, we first zeroed out signals resulting from electrical noise. We then perform a least-squares fitting routine to the curve

$$P \approx P_{\mathrm{nom}}\left(\frac{(t-t_0)e}{\alpha\tau}\right)^{\alpha} e^{(t_0-t)/\tau}, \tag{1}$$

with fit parameters t_0, τ, α, and P_{nom}.

This curve peaks at time $t_{\mathrm{pk}}=t_0+\alpha\tau$ and pressure P_{nom}. It has a single zero at t_0. We take the beginning and end of the pressure pulse to be at the 50% levels of the fitted curve. We will refer to the corresponding times as t_{rise} and t_{fall}. The data have significant scatter, but the leading edge travels at 110 km/s and the peak at 140 km/s. The tail appears simultaneously at all locations.[14] See Fig. 2 for a comparison of the raw and trimmed signals to this model. We plot the amplitude and timing of the pulses as functions of position in Figs. 3 and 4.

We use a two-fluid approximation and treat the ions and electrons as separate ideal gasses with the same temperature[14] $T\equiv T_e=T_i$. The fluid pressures of the two components are

$$P_{\mathrm{fluid},e} = n_e k_B T_e \tag{2}$$

and

$$P_{\mathrm{fluid},i} = n_i k_B T_i = n_e k_B T/Z. \tag{3}$$

The other factors in the equation are the electron and ion number densities n_e and n_i, Boltzmann's constant k_B, and the average ionization state $Z\approx n_e/n_i$.

If the pressure probe was flush with the chamber wall and the gas's specific heat capacity was independent of temperature, the probe would measure the adiabatic stagnation pressure (Ref. 16, p. 59). We calculate this specifically for the ion fluid:

$$P_{\mathrm{stag}} \approx P_{\mathrm{stag},i} = P_{\mathrm{fluid},i}\left[1+\frac{\gamma-1}{2}\left(\frac{v}{a}\right)^2\right]^{\gamma/(\gamma-1)}. \tag{4}$$

Although the ions will realistically have some coupling to the electron fluid, we ignore this for the moment[14] and use adiabatic indices $\gamma=\gamma_i=5/3$ and $\gamma_e=1$. We combine formulas from several different sources (Ref. 17, p. 29; Ref. 18, p. 263; and Ref. 19, p. 108) to obtain a general formula for the speed of sound a. This accounts for finite ion temperature and ionization state Z. We obtain

$$a^2 = \frac{k_B}{m_i}(ZT_e\gamma_e+\gamma_i T_i) \approx \frac{k_B T(Z+\gamma)}{m_i}, \tag{5}$$

which yields $a\approx12$ km/s. The electron stagnation pressure is much smaller than the ion pressure[14] and will be ignored. The temperature $T\approx3$ eV, ion mass $m_i\approx5$ amu, and ionization state $Z\approx1$ are based on spectroscopic measurements below.

[a]Electronic mail: messer@hyperv.com.

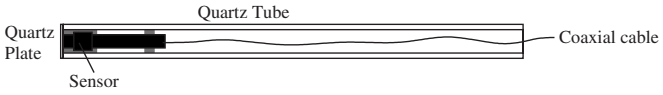

FIG. 1. Pressure probe in its housing. We attach a precision coaxial cable to a commercial sensor and slide the cable through a quartz tube. Epoxy and electrical tape bind the probe inside the tube. One side of a thin quartz disk is smeared with epoxy. This is used to push the sensor into its final position, assuring contact between the probe head and the quartz disk. The disk protects the sensor from the plasma.

By assuming that the measured pressure P_{nom} corresponds to the adiabatic stagnation pressure P_{stag}, we can check for consistency with other diagnostics. Visible-light imaging shows the plasma's arrival at the probe coincident with the steep rise on the pressure pulse. The image also shows a clear bow shock.

Several variables contributing to the stagnation pressure are measured by spectroscopy:[20] Doppler shifts indicate an overall plasma speed of $v \approx 90$ km/s. The observed carbon line ratios indicate an electron temperature of about 3 eV. Stark broadening and interferometry both measure electron densities n_e near 5×10^{20} m^{-3}. We also assume $Z \approx 1$, $T_i \approx T_e$, and $m_i \approx 5$ amu, all of which are consistent with the spectroscopy but which are not directly measured. We assume an ion mass of 5 amu since we have a polyethylene (CH_2) ablative plasma with a small admixture of higher-mass species. From these values, we expect a muzzle stagnation pressure (Eq. (4)) of approximately 350 kPa. This is slightly below the 380 kPa from the exponential fit curve through the $P_{\mathrm{nom}}(z)$ data (see Fig. 3). We assume that the spectroscopic numbers are accurate throughout this article, but note that spectroscopy must integrate over a larger volume and longer duration than the probe.

Measurements with a ballistic pendulum placed in the plasma stream[13,21] indicate a total momentum of about 13 g m/s at the muzzle. Using our standard 90 km/s velocity, we calculate a total plasma mass of 140 μg. This is a factor of 3–4 above what we estimate from other diagnostics.[14] For all our diagnostics, shot-to-shot variations exceed estimated uncertainties.

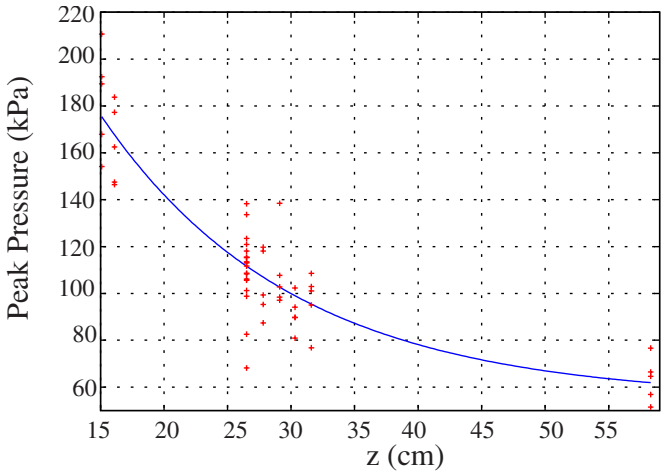

FIG. 3. (Color online) Characteristic height P_{nom} of pressure wave as a function of distance from the muzzle. Each point shows the pressure for a single shot. The curve is the optimum exponential fit, (330 kPa)$e^{-z/(15\ \mathrm{cm})}$ +55 kPa.

There are two distinct phenomena revealed by the pressure probe. We first describe the shock front then describe and analyze the global decrease in pressure.

The clearest aspect of our data is the propagation of a shock wave. The passage of the shock is shown by a sudden increase in pressure, with the time of the increase depending on the distance of the probe from the muzzle. A linear fit to arrival time (t_{rise}) versus position (z) gives an average speed of 110 km/s (see Fig. 4). Measurements at intermediate locations would allow a better description of possible slowing down. As expected,[16] the 90 km/s fluid velocity from spectroscopy is lower than the 110 km/s shock velocity from the pressure probe.

We do not analyze the leading edge of the pressure pulse in detail because of the negative swing in the measured pres-

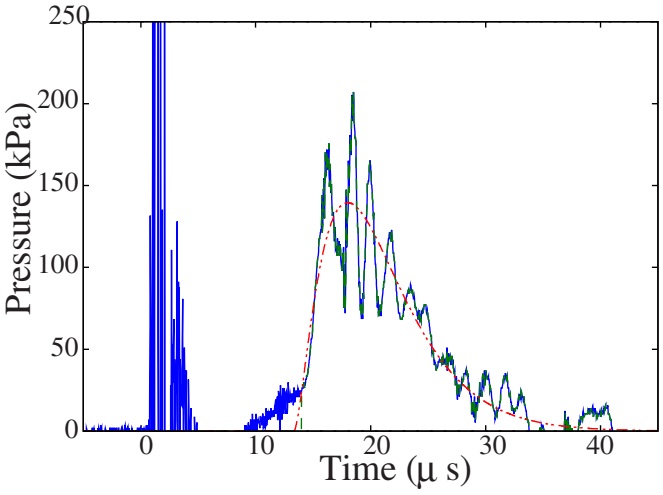

FIG. 2. (Color online) Sample pressure probe trace. We trim the raw signal (solid line) to remove the initial noise. The resulting curve (dashed, rising from zero near 13 μs) is fitted to Eq. (1) (dot-dot-dashed, smooth curve). Traces are compared based on the fitted curves.

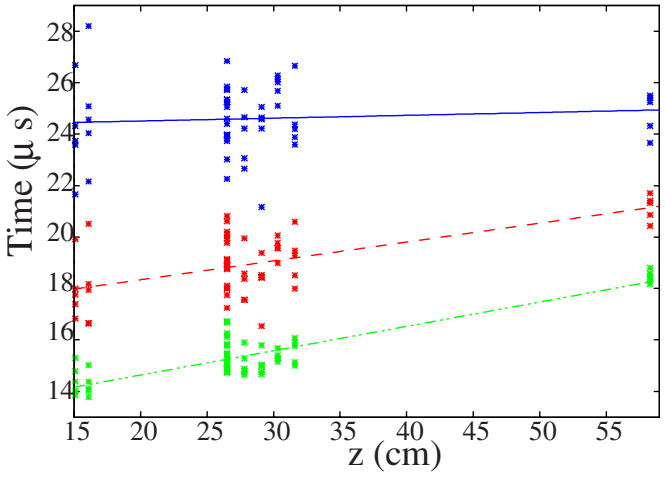

FIG. 4. (Color online) Pressure wave timing as a function of position. The lowest data set is arrival time t_{rise}. The middle data set shows the time t_{pk} of peak pressure. The top data set shows the time t_{fall} of the pressure decrease. Points show individual measurements. The lines are linear fits.

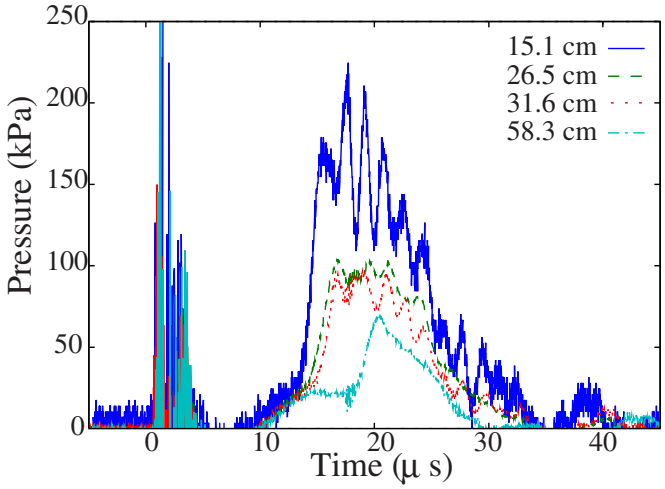

FIG. 5. (Color online) Averaged probe traces at four positions. The signals before 13 μs are dominated by noise. In particular, the slow rise visible before 13 μs appears even if the probe is outside the vacuum chamber. The rollover at 15 μs in the 58.3 cm trace is part of this electrical noise. The sharp rise between 12 and 20 μs occurs only when the probe faces into the flow. The 15.1 cm probe signal rises first and is the highest, followed by the 26.5 cm and 31.6 cm signals. The 58.3 cm is the last to appear and gives the weakest pressure.

sure and the gradual rise which follows it. This unphysical decrease and slow rise are observed only when the high voltage switches are closed and not during shock tube calibration. In addition, they are observed even when the probe is outside the vacuum chamber. In this case, the pressure signal rises only to a small positive value, and we therefore assume that the peak pressure is accurate.

The second phenomenon visible in the pressure data is that the pressure at all sampled positions decreases *simultaneously* within shot-to-shot variation (see Figs. 4 and 5). The pressure decrease is probably[14] due to cooling and recombining plasma. This hypothesis is constrained by the interferometry signal, which shows a decrease in the number of free electrons as the pressure decreases. Since the pressure decrease is nearly simultaneous at all measured positions, it may be that the latter part of the pressure signal is due to a thermal plasma filling the chamber. If so, the decrease is a result of both cooling and expansion. The interferometer signals show a time scale τ_n of about 5.8 μs for the density decrease,[22] compared to the $\tau_P \approx 2.8$ μs time scale for the decrease in the pressure signal on the same shots. This is consistent with adiabatic expansion of the plasma: A gas expanding adiabatically satisfies (Ref. 23, p. 17)

$$P = Cn^{\gamma} \tag{6}$$

for some constant C. The time derivative is

$$\dot{P} = \gamma C n^{\gamma-1} \dot{n}. \tag{7}$$

The ratio of these two equations gives the relative time constants $\tau_\chi \equiv \chi/\dot{\chi}$:

$$\frac{P}{\dot{P}} = \frac{n^{\gamma}}{\gamma n^{\gamma-1}\dot{n}} = \frac{n}{\gamma \dot{n}}, \tag{8}$$

$$\gamma \tau_P = \tau_n. \tag{9}$$

This implies that we have $\gamma \approx 2$, which is close to the nominal $\gamma = 5/3$. Once the plasma splashes off the back wall of the chamber, the axial kinetic energy will be redistributed over motion in all three dimensions. This will effectively increase the ion and electron thermal speeds to about $\sqrt{v^2/3 + v_T^2}$. (v_T is the species-dependent thermal speed before impact.) Only the electrons travel fast enough for their effects to appear simultaneous in our data set.[14] Because all probe positions show simultaneous pressure decreases, we suspect that the electrons keep all postimpact plasma at essentially the same temperature. Because the ions are much more massive and slower, gradients in mass density persist on the cooling time scales, leading to the observed dependence of pressure on position. We expect corresponding variations in electron density to maintain quasineutrality. It is not clear what causes this density gradient, but it presumably depends on details of the stagnation process.

We have made preliminary measurements of the stagnation pressure of the plasma plume produced by a coaxial gun which has since been installed at the Maryland Centrifugal Experiment. The pressure probe signals are roughly consistent with measurements of plasma parameters from other diagnostics and with the assumption of adiabatic compression when the plasma impacts the probe tip. There is clear evidence for a pressure front with a muzzle shock velocity near 110 km/s and a fluid velocity near 90 km/s. The adiabatic stagnation pressure near the muzzle is about 190 kPa and decreases with distance downstream. There are, however, several unknowns[14] regarding the precise interpretation of the pressure signals. We plan to take additional measurements so that we may add more detailed pressure data to our description, as well as provide tighter comparisons to other diagnostics. Spectroscopy, interferometry, and magnetic probes are currently producing data, and we are looking for ways to improve these diagnostics. We also plan to add a laser deflectometer over the course of the coming year and to do more simulations to assist the interpretation of these data.

The authors would like to acknowledge help by Dr. Tom York, who donated an initial pressure probe and calibration shock tube and who provided invaluable advice on building additional probes and a second shock tube. Dr. Ray Elton has also been very helpful in the collection and interpretation of spectroscopic data. We would also like to thank Dr. Sam Brockington for his critique of several drafts of this manuscript. This work was supported by the U.S. DOE Office of Fusion Energy Sciences Contract No. DE-FG02–05ER54810.

[1] J. Marshall, Phys. Fluids **3**, 134 (1960).
[2] K. Thom, J. Norwood, and N. Jalufka, Phys. Fluids **7**, S67 (1964).
[3] A. V. Voronin and K. G. Hellblom, Plasma Phys. Controlled Fusion **43**, 1583 (2001).
[4] A. V. Voronin, V. K. Gusev, Yu. V. Petrov, N. V. Sakharov, K. B. Abramova, E. M. Sklyarova, and S. Yu. Tolstyakov, Nucl. Fusion **45**, 1039 (2005).
[5] T. E. Markusic, Y. C. F. Thio, and J. T. Cassibry, *Proceedings of the 38th AIAA/ASME/SAE/ASEE Joint Propulsion Conference*, Indianapolis, IN, 2002 (American Institute of Aeronautics and Astronautics, Reston, VA, 2002), AIAA Paper No. 2022-4125.

[6]T. M. York, C. Zakrzwski, and G. Soulas, J. Propul. Power **9**, 553 (1993).
[7]C. J. Michels and T. M. York, AIAA J. **11**, 579 (1973).
[8]S. Woodruff, D. N. Hill, B. W. Stallard, R. Bulmer, B. Cohen, C. T. Holcomb, E. B. Hooper, H. S. McLean, J. Moller, and R. D. Wood, Phys. Rev. Lett. **90**, 095001 (2003).
[9]S. J. Howard, "Interaction dynamics of high Reynolds number magnetized plasma flow on the CTIX plasma accelerator," Ph.D. thesis, University of California, Davis, 2006.
[10]J. T. Cassibry, Y. C. F. Thio, and S. T. Wu, Phys. Plasmas **13**, 053101 (2006).
[11]K. L. Baker, D. Q. Hwang, R. W. Evans, R. D. Horton, H. S. McLean, S. D. Terry, S. Howard, and C. J. DiCaprio, Nucl. Fusion **42**, 94 (2002).
[12]K. L. Baker, R. D. Horton, D. Q. Hwang, R. W. Evans, and S. Howard, IEEE Trans. Plasma Sci. **30**, 48 (2002).
[13]F. D. Witherspoon, A. Case, S. J. Messer, R. Bomgardner III, M. W. Phillips, S. Brockington, and R. Elton, "A contoured gap coaxial plasma gun with injected plasma armature," Rev. Sci. Instrum. (unpublished).
[14]See EPAPS Document No. E-PHPAEN-16-045906 for detailed calculations and procedures concerning probe calibration and additonal data in support of the models used here. For more information on EPAPS, see http://www.aip.org/pubservs/epaps.html.
[15]G. Persico, P. Gaetani, and A. Guardone, Meas. Sci. Technol. **16**, 1751 (2005).
[16]J. D. Anderson, Jr., *Modern Compressible Flow with Historical Perspective*, 2nd ed. (McGraw-Hill, New York, 1990).
[17]*NRL Plasma Formulary*, edited by J. D. Huba (Naval Research Laboratory, Washington, DC, 2002), Naval Research Laboratory Report No. NRL/PU/6790-02-450, 2002.
[18]R. J. Goldston and P. H. Rutherford, *Introduction to Plasma Physics* (Institute of Physics Publishing, Philadelphia, 1995).
[19]N. A. Krall and A. W. Trivelpiece, *Principles of Plasma Physics* (McGraw-Hill, New York, 1973).
[20]A. Case, F. D. Witherspoon, S. J. Messer, R. Bomgardner, M. W. Phillips, D. Van Doren, R. Elton, and I. Uzun-Kaymak, Bull. Am. Phys. Soc. **52**, 250 (2007).
[21]S. Messer, F. D. Witherspoon, R. Bomgardner, A. Case, M. W. Phillips, and D. Van Doren, Bull. Am. Phys. Soc. **52**, 250 (2007).
[22]A. Case, S. Messer, R. Bomgardner, and F. D. Witherspoon, "Interferometer density measurements of a high-velocity plasmoid," Phys. Plasmas. (to be published).
[23]R. K. Pathria, *Statistical Mechanics* (Butterworth-Heinemann, Boston, 1998).